Published in final edited form as:
Ann Thorac Surg. 2015 February ; 99(2): 597–603. doi:10.1016/j.athoracsur.2014.09.014.

Injectable Microsphere Gel Progressively Improves Global Ventricular Function, Regional Contractile Strain, and Mitral Regurgitation after Myocardial Infarction

Jeremy R McGarvey, MD[1], **Norihiro Kondo, MD**[1], **Walter RT Witschey, PhD**[1,2], **Manabu Takebe, MD**[1], **Chikashi Aoki, MD**[1], **Jason A. Burdick, PhD**[3], **Francis G Spinale, MD, PhD**[4], **Joseph H Gorman III, MD**[1], **James J Pilla, PhD**[1,2], and **Robert C Gorman, MD**[1]

[1]Gorman Cardiovascular Research Group, Department of Surgery, University of Pennsylvania

[2]Department of Radiology, University of Pennsylvania

[3]Department of Bioengineering, University of Pennsylvania

[4]University of South Carolina School of Medicine

Abstract

Background—There is continued need for therapies which reverse or abate the remodeling process following myocardial infarction (MI). In this study, we evaluate the longitudinal effects of calcium hydroxyapatite microsphere gel on regional strain, global ventricular function, and mitral regurgitation (MR) in a porcine MI model.

Methods—Twenty five Yorkshire swine were enrolled. Five were dedicated weight-matched controls. Twenty underwent posterolateral infarction by direct ligation of the circumflex artery and its branches. Infarcted animals were randomly divided into four groups: one week treatment, one week control, four week treatment, and four week control. Following infarction, animals received either twenty 150μl calcium hydroxyapatite gel or saline injections within the infarct. At their respective timepoints, echocardiograms, cardiac MRI, and tissue were collected for evaluation of MR, regional and global left ventricular function, wall thickness, and collagen content.

Results—Global and regional LV function were depressed in all infarcted subjects at one week compared to healthy controls. By four weeks post-infarction, global function had significantly improved in the calcium hydroxyapatite group compared to infarcted controls (EF 48.5±1.9% vs. 38.0±1.7%, $p<0.01$). Similarly, regional borderzone radial contractile strain (16.3±1.5% vs. 11.2±1.5%, $p=0.04$), MR grade (0.4±0.2 vs. 1.2±0.2, $p=0.04$), and infarct thickness (7.8±0.5mm vs. 4.5±0.2mm, $p<0.01$) were improved at this timepoint in the treatment group compared to infarct controls.

Corresponding Author: Robert C Gorman, MD, Gorman Cardiovascular Research Group, Smilow Center for Translation Research, 3400 Civic Center Blvd, 11-114, Philadelphia, PA 19104-5156, robert.gorman@uphs.upenn.edu.

Conclusions—Calcium hydroxyapatite injection following MI progressively improves global LV function, borderzone function, and mitral regurgitation. Using novel biomaterials to augment infarct material properties is viable alternative in the current management of heart failure.

Keywords

Biomaterials; Heart Failure; MRI; Myocardial Mechanics; Myocardial Remodeling

Introduction

Myocardial infarction (MI) precipitates approximately 70% of heart failure cases, and population modeling suggests the prevalence of both coronary artery disease and heart failure will further increase in the coming decades [1,2]. Progressively increasing scar compliance results in infarct expansion, which leads to impaired borderzone contraction, significant left ventricular (LV) systolic dysfunction and ventricular dilatation [3,4]. Passive restraint devices have been previously shown to limit the infarct expansion, improve borderzone function and ameliorate LV remodeling [5–12]. Unfortunately, application of such devices thus far has been limited by technical concerns and risk profiles from early clinical trials[13].

Injectable acellular biomaterials designed reverse or abate the remodeling process are of interest to surgeons and interventionalists as potential new treatment modalities in the limited armamentarium against ischemic cardiomyopathy. These therapies can potentially provide a minimally invasive and technically straightforward means of attenuating infarct expansion by directly providing structural support and/or by favorably altering the endogenous wound healing response in the infarct [14–18].

Radiesse® is a commercially available soft tissue filler gel composed of 30% 25–45μm calcium hydroxyapatite microspheres suspended in 70% water, glycerin, and carboxymethylcellulose and has been utilized for a variety of cosmetic and reconstructive applications [19]. Injection of the material induces neocollagenesis by inducing a phenotypic shift in wound-infiltrating macrophages from a pro-inflammatory phenotype towards and anti-inflammatory/pro-healing phenotype [20,21].

We have previously shown using 3-dimensional echocardiography that epicardial injection of Radiesse® following apical MI increases infarct stiffness, reduces infarct expansion and limits global LV remodeling [22,23]. Using a novel 3-dimensional tagged cardiac MRI, this study extends our previous work by evaluating the spatiotemporal effects of Radiesse® injection on regional contractile strains and global post-infarct ventricular function as well as mitral valve function in a large animal posterolateral infarct model.

Material and Methods

The longitudinal effects of calcium hydroxyapatite microsphere injection (Radiesse®) on global LV and borderzone function were studied in a porcine infarct model.

With approval from The University of Pennsylvania's Institutional Animal Care and Use Committee, twenty five male Yorkshire swine weighing 37.2±1.2kg were enrolled in this study. Twenty subjects underwent posterolateral infarction by direct coronary artery ligation via left thoracotomy. These animals were then randomized to sham injection or hydroxyapatite injection groups—with ten subjects per treatment. Post-infarct animals were then allowed to survive for either one or four weeks, at which point they underwent terminal imaging and tissue preparation. Five additional animals were used as healthy weight-matched controls. All studies were performed in compliance with the Guide for the Care and Use of Laboratory Animals (National Institutes of Health Publication no 85-23, revised 1996).

Infarction and Injection

All animals—with exception of healthy controls— underwent posterolateral infarction via left thoracotomy. Subjects were first sedated with intramuscular ketamine injection (25–30mg/kg), intubated, and mechanically ventilated. General anesthesia was maintained on mixed isoflorane (1.5–3.0%) and oxygen, which was delivered by volume-controlled ventilation (tidal volume 10–15mg/kg). Aseptic technique was maintained throughout each procedure. Via left thoracotomy, animals underwent selective ligation of the circumflex artery and/or its branches with nonabsorbable polypropylene suture to create a posterolateral infarct involving approximately 15–18% of the LV. Akinesis of the involved wall was confirmed with intraoperative echocardiography. Ten custom 2mm platinum markers were positioned around the infarct periphery to assist in infarct localization during later MRI acquisitions and postprocessing.

Thirty minutes after infarction, animals were randomized to infarct control or treatment (Radiesse®) groups. Subjects then received twenty evenly distributed 150μl injections of either 0.9% normal saline (infarct control) or Radiesse® (treatment) throughout the infarct area. Hemodynamic and echocardiographic data was recorded pre-infarction, post-infarction, and post-injection. After ensuring hemodynamic and electrophysiologic stability, all animals were then recovered. Subjects were then sub-divided into either one week or four week timepoints (N=5 per treatment/timepoint).

MRI

All animals, including healthy controls, underwent cardiac MRI to assess global ventricular function, 3D strain, and wall thickness. General anesthesia was maintained for the entirety of the imaging procedures, as described above. A high-fidelity pressure transduction catheter (Millar Instruments; Houston, TX) was positioned for LV pressure gating. MRI was performed using a 3T Seimens Trio A Tim Magnetom scanner (Seimens; Malvern, PA). Animals underwent prospectively-gated 3D SSFP cine MRI for volumetric analysis using the following parameters: field of view – 300 × 244, acquisition matrix – 192 × 156, repetition time – 3.11ms, echo time – 1.53ms, bandwidth – 1184Hz/pixel, slice thickness – 4mm, averages – 2. Regional LV strain was assessed using a 3D SPAMM (SPAtial Modulation of Magnetization) tagged sequence with the following parameters: field of view – 260 × 260, acquisition matrix – 256 × 128, repetition time – 34.4ms, tag spacing – 6mm, bandwidth 330Hz/pixel, slice thickness – 2mm, averages – 4. Fifteen minutes following

intravenous injection of 0.1mmol/kg gadobenatedimeglumine (MultiHance; Bracco Diagnostics, Princeton, NJ), infarct location and wall thickness were visualized using a 3D late-gadolinium enhanced (LGE) spoiled gradient echo sequence with the following parameters: field of view – 350 × 350, acquisition matrix – 256 × 256, repetition time – 591.28ms, echo time – 2.96ms, inversion time – 200–300ms, flip angle - 25°, averages – 2. Images were archived and stored off-line for post-processing.

Echocardiography

Prior to euthanasia, all animals underwent epicardial 2-D and 3-D Doppler echocardiography using a 2- to 7-MHz matrix array transducer (Philips Medical Systems iE33, Andover, MA, USA) for assessment of mitral regurgitation (MR). Images were stored off-line for analysis. The severity of mitral regurgitation (MR) was assessed semi-quantitatively on the standard 0–4 scale by two analysts blinded to treatment group [24]. Average scores for each subject were then compared between control and treatment groups for each timepoint.

Image Post-Processing

Imaging data sets were blinded to the end-user throughout post-processing.

LV volume and global function data was obtained using prospective SSFP cine MRI images. Raw short-axis images were automatically sorted, cropped and contrast normalized in a custom Matlab (Natick, MA) program to ensure homogenous LV coverage and image quality, respectively. Segmentation was then performed through all cardiac phases of the sorted and correct images using a semi-automated 3D active contour segmentation program (ITK-SNAP, open access/source) [25]. LV end-diastolic volume (EDV), end-systolic volume (ESV), stroke volume (SV), and ejection fraction (EF) were then computed throughout the entire cardiac cycle from segmented images using in-plane and through-plane spatial resolution information.

Regional strain measurements were calculated from 3D SPAMM acquisitions using an optical flow technique. Epicardial and endocardial contours were first manually segmented at the end diastolic reference state using ImageJ software (NIH; Bethesda, MD). Image masks were created from segmented contours to isolate LV myocardium. A custom optical flow plug-in for ImageJ was used to derive 3D displacement flow fields from the stacked images through end-systole [26]. Using a custom Matlab program, infarct boundaries were identified using the previously placed platinum epicardial markers and LGE landmarks. Using a centroid placed within the LV, Borderzone myocardium was then automatically defined by the region extending 20 degrees beyond the infarct boundaries on each side [9]. Remote regions were automatically defined as the regions extending 40 degrees beyond the borderzone boundaries on each side. The endocardial and epicardial edges were excluded to reduce noise from blood and lung movement, respectively. Maximum principle strain (ε_{max}) —indicative of contractile function due to LV wall thickening—was then calculated for each region and 3D strain maps were generated (Figure 1a).

Infarct wall thickness was measured from LGE MRI images at end diastole (Figure 1b–e). Thirty random radially-oriented spokes were positioned throughout each 3D infarct area.

Platinum markers and LGE images were used to confirm infarct boundaries. Average thickness was computed from spoke length.

Tissue Analysis

Infarct size was measured by planimetry from the endocardial infarct surface area using ImageJ image analysis software. Tissue was then stained for collagen content using PSR staining.

Statistics

All data is presented as mean ± standard error of the mean (SEM). Volumetric, strain, and infarct wall thickness comparisons were performed using unpaired two-tailed *t* tests. A p value less than 0.05 was considered statistically significant.

Results

All animals successfully underwent infarction and reached their respective end-points with no unexpected deaths. No adverse outcomes, such as post-operative arrhythmia or material embolism, were encountered.

Global Ventricular Function

At one week following posterolateral infarct, both infarct control and Radiesse® treated animals developed significant reduction in ejection fraction compared to healthy control (EF 55.8±5.4% versus 38.5±2.4% infarct control versus 38.3±1.9% Radiesse® treated, $p<0.01$) (Figure 2). At this timepoint, ESV increased from 25.4±6.3ml in healthy animals to 46.0±4.8ml ($p=0.02$) in infarct controls and 46.6±3.4ml ($p=0.01$) in Radiesse® treated animals. Similarly, EDV increased from 54.5±6.4ml in healthy controls to 74.0±5.6ml ($p=0.05$) in infarct controls and 75.6±4.8ml ($p=0.02$). SV was similar among healthy controls (29.1±1.1ml), infarct controls (27.9±1.5ml, $p=0.59$), and Radiesse® treated (28.9±2.2ml, $p=0.95$). There were no differences in volumes or global function noted between treatment groups at one week.

At four weeks following posterolateral infarct, infarct control animals showed progressive dilation and loss of systolic function, while Radiesse® treated animals demonstrated improvement of all indices towards healthy control levels. EF following Radiesse® treatment improved to 48.5±1.9% ($p=0.20$ compared to healthy control), while infarct control EF remained reduced at 38.0±1.7% ($p<0.01$ versus 4wks post-Radiesse® treatment and healthy control). ESV significantly improved at four weeks in the Radiesse® treated group (38.6±2.1ml Radiesse® versus 54.3±3.3ml infarct control, $p<0.01$). Infarct only animals showed progressive dilation of the ventricle at four weeks compared to Radiesse® treated animals, which maintained EDV similar to one week (74.7±2.9ml Radiesse® versus 87.4±3.9ml infarct control, $p=0.03$). SV was preserved between infarct control and Radiesse® treated animals at four weeks post-infarct (36.2±1.8ml Radiesse® versus 33.1±1.6ml infarct control, $p=0.22$).

Regional Ventricular Function

Remote and borderzone regional maximal principle strain was reduced in all infarct animals relative to uninfarcted healthy controls; however, maximal principle strain was improved in Radiesse® treated animals at both one week and four week timepoints compared to infarct controls (Figure 3). Healthy animal control posterolateral radial wall strain was 16.2±1.4%. At one week, remote myocardial strain was 11.9±0.8% in untreated infarct controls and 13.7±2% in Radiesse® treated animals ($p=0.05$ between infarct and healthy controls, $p=0.32$ between Radiesse® treatment and healthy controls, and $p=0.44$ between infarcted groups). Similarly, borderzone radial strain at one week was 9.4±0.7% in infarct controls versus 11.1±1.6% following Radiesse® treatment ($p<0.01$ between infarct and healthy controls, $p=0.04$ between Radiesse® treatment and healthy controls, and $p=0.38$ between infarct groups).

At four weeks post-infarction, regional maximal principle strain following Radiesse® treatment continued to improve to near healthy control levels, while untreated infarct controls remained depressed. Remote regional strain at four weeks was 12.8±1.1% among infarct controls and 15.9±1.4% in Radiesse® treated infarcts ($p=0.11$ between infarct and healthy controls, $p=0.89$ between Radiesse® treatment and healthy controls, and $p=0.11$ between infarct groups). Borderzone regional strain was 11.2±1.5% in infarct controls and 16.3±1.5% in the Radiesse® group ($p=0.03$ between infarct and healthy controls, $p=0.96$ between Radiesse® treatment and healthy controls, and $p=0.04$ between treatment groups).

Mitral Regurgitation

At one week post-infarction, there was no difference in severity of MR between control and treatment groups (1.0±0.0 vs 0.8±0.4, respectively). At four weeks post-infarction, there was improvement in the grade of MR from 0.4±0.2 with Radiesse® treatment to 1.2±0.2 in the control arm ($p=0.04$).

Infarct Size, Thickness and Histology

In vivo infarct wall thickness generated from MRI cine images demonstrated progressive thickening of Radiesse® treated infarcts, while untreated infarct controls thinned (Figure 2, right axis). Healthy control posterolateral myocardial wall thickness at end diastole was 7.4±0.3mm. At one week post-infarct, Radiesse® treated and untreated infarct controls wall thickness were similar—6.3±0.5mm versus 5.7±0.2mm ($p=0.34$), respectively. By four weeks post-infarct, Radiesse® treated infarcts thickened to 7.8±0.5mm while infarct control wall thickness decreased to 4.5±0.2mm ($p<0.001$ between groups). This finding also represented a significant increase in wall thickness for Radiesse® treated animals from one week to four weeks ($p=0.05$), and a significant decrease in untreated infarct controls ($p<0.01$).

PSR collagen staining of infarct tissue qualitatively found dense collagen islands and cellular infiltrates surrounding Radiesse® microsphere islands compared to untreated infarct controls (Figure 4). Untreated control tissue at one week demonstrates homogenous faint collagen staining, which is slightly more pronounced by four weeks. Radiesse® treated

animals show dense collagen depositions around calcium hydroxyapatite islands which appear more dense and organized by four weeks.

Infarct size was similar between all treatment groups by planimetry—with one week control, one week Radiesse® treated, four week control, and four week Radiesse® treated infarcts measuring 15.7±1.2%, 15.3±0.8%, 15.3±0.6%, and 16.6±0.7% of total LV surface area respectively ($p>0.05$).

Comment

Epicardial injection of calcium hydroxyapatite microspheres shortly after posterolateral infarction ameliorated LV dilatation and was associated with progressive improvement in both borderzone and global LV function compared to sham controls. These findings were accompanied by reduced infarct thinning in the treatment group. At one week post-infarction, no significant differences were found between groups. Both treated and untreated infarct control groups showed evidence of immediate LV dilatation and systolic dysfunction compared to healthy controls at this timepoint. By four weeks, however, the Radiesse® treatment group had not experienced infarct thinning and demonstrated near normalization of global function and borderzone contractile strain, while saline treated subjects showed regional and global evidence of on-going LV remodeling with infarct thinning. Similarly, MR was improved in the four week Radiesse® treated group compared to controls.

Although both groups demonstrated signs of early adverse remodeling, the untreated infarct group experienced persistent adverse remodeling between 1 week and 4 weeks after MI, while further LV dilation was prevented in the treatment group as global and regional contractile function nearly normalized. Radiesse® remains one of the stiffest injectable biomaterials commercially available for medical purposes [27], and the viscoelastive properties of this gel were the primary reason for its selection in this study. These temporal differences indicate that the beneficial effect was most likely the result of a biologic response to the injectate rather than mechanical characteristics of the material. Microsphere-based biomaterials have been found to alter the phenotype of macrophages and fibroblast responding to healing wounds. Recent work by our group is supportive of this hypothesis—showing temporal changes in fibroblast function and differentiation following Radiesse® injection with increased proliferation and migration of myofibroblasts [15,16,21].

These findings also corroborate earlier echocardiographic studies showing improved LV function after Radiesse® injection in an apical infarct model[22,23]. The current study extends our previous work by demonstrating that the prevention of infarct expansion by Radiesse® also improves borderzone contractile function and prevents extension of contractile dysfunction to progressively larger regions of perfused myocardium. Progressive increases in borderzone stress distributions following MI are thought to contribute to global contractile dysfunction and clinical heart failure symptoms [4,28–31]. This study supports that hypothesis. By augmenting infarct wall material properties, we can provide a more robust substrate upon which normally perfused borderzone can contract. Accordingly, we further hypothesize that the favorable effects seen after Radiesse® injection in this study are likely secondary to progressive infarct stiffening and resulting stabilization of the

borderzone myocardium and nearby papillary muscles—effects which are corroborated by progressive infarct wall thickness and the potential to limit development of ischemic mitral regurgitation.

In spite of revascularization treatments, over one third of patients with MI will later develop heart failure symptoms [32] —emphasizing the need for new therapeutic options. With a trend towards less-invasive treatment modalities, localized ventricular restraint/stiffening devices and injectable biomaterials have gained considerable clinical and research interest in the secondary prevention of heart failure [5,10,11,14,33,34]. While this study focuses on a single treatment, our group and others are actively involved in the development of other catheter-based therapeutics which are designed to alter the biochemical milieu and/or LV material properties [15–18,35,36]. An acknowledged limitation of Radiesse® injection is its inability to be injected via catheter due to high viscosity—necessitating open epicardial injections. In future studies, we plan on utilizing both shear thinning hydrogels and bioactive materials to alter post-infarct remodeling mechanics via a catheter-based approach [37,38].

In vivo quantification of therapeutic efficacy is typically limited to more traditional imaging techniques to date (e.g. echocardiography). Such modalities are often limited in spatial, dimensional or temporal resolution and provide limited insight into subtle regional function. In this study, we employed the use of high-spatial and temporal resolution 3D tagged cardiac MRI techniques to measure regional contractile wall strain (ε_{max}) following biomaterial injection. Progressively increased systolic borderzone strain in the treatment groups compared to control supports the notion that infarct thinning and increased wall compliance drives LV remodeling. Nonetheless, borderzone wall strain and global LV function are indirect measures of *in vivo* infarct wall compliance and stress—metrics which have traditionally required *ex vivo* biaxial tissue analysis [3]. With the use of finite element modeling combined with diastolic 3D tagged cardiac MRI, our group is currently validating a technique by which LV wall stress-strain relationships can be directly quantified *in vivo* [17,39]. Additionally, MRI-based studies focused on long-term assessment of infarct stress-strain relationships following acellular biomaterial injection are currently in process. In these studies, we are also implementing 4-D velocity-encoded MRI flow analysis to quantitatively assess mitral regurgitant fraction as well as LV diastolic fluid dynamics following biomaterial injection.

In conclusion, we have shown progressive improvement in global ventricular function, regional borderzone strain, and mitral regurgitation following directed injection of calcium hydroxyapatite microspheres into infarcted myocardium. These findings support the role of biomaterials in the treatment of ischemic cardiomyopathy. Further, high-resolution 3D MRI imaging techniques are emerging as an important tool in the measurement of therapeutic efficacy and *in vivo* biomechanics.

Acknowledgments

Supported by grants (HL63954, HL73021, and HL103723) from the National Heart, Lung, and Blood Institute of the National Institutes of Health, Bethesda, MD, USA

References

1. Goa S, Mozaffarian D, Roger VL, et al. Heart Disease and Stroke Statistics--2014 Update: A Report From the American Heart Association. Circulation. 2013:1–267.
2. Heidenreich PA, Trogdon JG, Khavjou OA, et al. Forecasting the future of cardiovascular disease in the United States: a policy statement from the American Heart Association. Circulation. 2011:933–44. [PubMed: 21262990]
3. Gupta KB, Ratcliffe MB, Fallert MA, et al. Changes in passive mechanical stiffness of myocardial tissue with aneurysm formation. Circulation. 1994; 89:2315–26. [PubMed: 8181158]
4. Jackson BM, Gorman JH, Moainie SL, et al. Extension of borderzone myocardium in postinfarction dilated cardiomyopathy. J Am Coll Cardiol. 2002 Sep 18; 40(6):1160–7. discussion 1168–71. [PubMed: 12354444]
5. Koomalsingh KJ, Witschey WRT, McGarvey JR, et al. Optimized local infarct restraint improves left ventricular function and limits remodeling. Ann Thorac Surg. 2013 Jan; 95(1):155–62. [PubMed: 23146279]
6. Blom AS, Mukherjee R, Pilla JJ, et al. Cardiac support device modifies left ventricular geometry and myocardial structure after myocardial infarction. Circulation. 2005; 112:1274–83. [PubMed: 16129812]
7. Blom AS, Pilla JJ, Arkles J, et al. Ventricular Restraint Prevents Infarct Expansion and Improves Borderzone Function After Myocardial Infarction: A Study Using Magnetic Resonance Imaging, Three-Dimensional Surface Modeling, and Myocardial Tagging. Ann Thorac Surg. 2007; 84:2004–10. [PubMed: 18036925]
8. Pilla JJ, Blom AS, Brockman DJ, et al. Ventricular constraint using the acorn cardiac support device reduces myocardial akinetic area in an ovine model of acute infarction. Circulation. 2002; 106:I207–I211. [PubMed: 12354735]
9. Pilla JJ, Blom AS, Gorman JH, et al. Early postinfarction ventricular restraint improves borderzone wall thickening dynamics during remodeling. Ann Thorac Surg. 2005; 80:2257–62. [PubMed: 16305885]
10. Magovern JA. Experimental and clinical studies with the Paracor cardiac restraint device. Semin Thorac Cardiovasc Surg. 2006; 17:364–8. [PubMed: 16428045]
11. Magovern JA, Teekell-Taylor L, Mankad S, et al. Effect of a flexible ventricular restraint device on cardiac remodeling after acute myocardial infarction. ASAIO J. 52(2):196–200. [PubMed: 16557108]
12. Enomoto Y, Gorman JH, Moainie SL, et al. Early ventricular restraint after myocardial infarction: extent of the wrap determines the outcome of remodeling. Ann Thorac Surg. 2005 Mar; 79(3): 881–7. discussion 881–7. [PubMed: 15734399]
13. FDA Circulatory Systems Advisory Panel. FDA REVIEW MEMORANDUM - CorCap® Cardiac Support Device (CSD) [Internet]. 2006
14. Burdick, Ja; Mauck, RL.; Gorman, JH., et al. Acellular biomaterials: an evolving alternative to cell-based therapies. Sci Transl Med. 2013; 5:176ps4.
15. Eckhouse SR, Purcell BP, McGarvey JR, et al. Local Hydrogel Release of Recombinant TIMP-3 Attenuates Adverse Left Ventricular Remodeling After Experimental Myocardial Infarction. Sci Transl Med. 2014 Feb 12.6(223):223ra21.
16. Purcell BP, Lobb D, Charati MB, et al. Injectable and bioresponsive hydrogels for on-demand matrix metalloproteinase inhibition. Nat Mater. 2014 Mar 30. advance on.
17. Kichula ET, Wang H, Dorsey SM, et al. Experimental and Computational Investigation of Altered Mechanical Properties in Myocardium after Hydrogel Injection. Ann Biomed Eng. 2013 Nov 23.
18. Macarthur JW, Cohen JE, McGarvey JR, et al. Preclinical evaluation of the engineered stem cell chemokine stromal cell-derived factor 1α analog in a translational ovine myocardial infarction model. Circ Res. 2014; 114:650–9. [PubMed: 24366171]
19. Kontis TC. Contemporary review of injectable facial fillers. JAMA Facial Plast Surg. 2013; 15:58–64. [PubMed: 23183718]

20. Coleman KM, Voigts R, DeVore DP, et al. Neocollagenesis after injection of calcium hydroxylapatite composition in a canine model. Dermatol Surg. 2008 Jun; 34(Suppl 1):S53–5. [PubMed: 18547182]
21. McGarvey JR, Pettaway S, Shuman J, et al. Targeted Injection of a Biocomposite Material Alters Macrophage and Fibroblast Phenotype and Function Following Myocardial Infarction: Relation to LV Remodeling. J Pharmacol Exp Ther. 2014 Jul 14.
22. Ryan LP, Matsuzaki K, Noma M, et al. Dermal filler injection: a novel approach for limiting infarct expansion. Ann Thorac Surg. 2009 Jan; 87(1):148–55. [PubMed: 19101288]
23. Morita M, Eckert CE, Matsuzaki K, et al. Modification of infarct material properties limits adverse ventricular remodeling. Ann Thorac Surg. 2011 Aug; 92(2):617–24. [PubMed: 21801916]
24. Miyatake K, Izumi S, Okamoto M, et al. Semiquantitative grading of severity of mitral regurgitation by real-time two-dimensional Doppler flow imaging technique. J Am Coll Cardiol. 1986; 7:82–8. [PubMed: 3941221]
25. Yushkevich PA, Piven J, Hazlett HC, et al. User-guided 3D active contour segmentation of anatomical structures: Significantly improved efficiency and reliability. Neuroimage. 2006; 31:1116–28. [PubMed: 16545965]
26. Xu C, Pilla JJ, Isaac G, et al. Deformation analysis of 3D tagged cardiac images using an optical flow method. J Cardiovasc Magn Reson. 2010 Jan.12:19. [PubMed: 20353600]
27. Kimura M, Mau T, Chan RW. Viscoelastic properties of phonosurgical biomaterials at phonatory frequencies. Laryngoscope. 2010 Apr; 120(4):764–8. [PubMed: 20213661]
28. Weisman HF, Bush DE, Mannisi JA, et al. Global cardiac remodeling after acute myocardial infarction: a study in the rat model. J Am Coll Cardiol. 1985; 5:1355–62. [PubMed: 3158687]
29. Jackson BM, Gorman JH, Salgo IS, et al. Border zone geometry increases wall stress after myocardial infarction: contrast echocardiographic assessment. Am J Physiol Heart Circ Physiol. 2003; 284:H475–H479. [PubMed: 12414441]
30. Kramer CM, Lima JA, Reichek N, et al. Regional differences in function within noninfarcted myocardium during left ventricular remodeling. Circulation. 1993; 88:1279–88. [PubMed: 8353890]
31. Epstein FH, Yang Z, Gilson WD, et al. MR tagging early after myocardial infarction in mice demonstrates contractile dysfunction in adjacent and remote regions. Magn Reson Med. 2002; 48:399–403. [PubMed: 12210951]
32. Hellermann JP, Goraya TY, Jacobsen SJ, et al. Incidence of heart failure after myocardial infarction: is it changing over time? Am J Epidemiol. 2003; 157:1101–7. [PubMed: 12796046]
33. McGarvey JR, Kondo N, Takebe M, et al. Directed epicardial assistance in ischemic cardiomyopathy: Flow and function using cardiac magnetic resonance imaging. Annals of Thoracic Surgery. 2013:577–85. [PubMed: 23810178]
34. Lee LS, Ghanta RK, Mokashi SA, et al. Optimized ventricular restraint therapy: Adjustable restraint is superior to standard restraint in an ovine model of ischemic cardiomyopathy. J Thorac Cardiovasc Surg. 2013; 145:824–31. [PubMed: 22698557]
35. Ifkovits JL, Tous E, Minakawa M, et al. Injectable hydrogel properties influence infarct expansion and extent of postinfarction left ventricular remodeling in an ovine model. Proc Natl Acad Sci U S A. 2010; 107:11507–12. [PubMed: 20534527]
36. Seif-Naraghi SB, Singelyn JM, Salvatore MA, et al. Safety and efficacy of an injectable extracellular matrix hydrogel for treating myocardial infarction. Sci Transl Med. 2013 Feb 20.5(173):173ra25.
37. Rodell CB, Kaminski AL, Burdick Ja. Rational Design of Network Properties in Guest-Host Assembled and Shear-Thinning Hyaluronic Acid Hydrogels. Biomacromolecules. 2013:1–7. [PubMed: 23157442]
38. Lu HD, Soranno DE, Rodell CB, et al. Secondary Photocrosslinking of Injectable Shear-Thinning Dock-and-Lock Hydrogels. Adv Healthc Mater. 2013:1–9.
39. Wenk JF, Eslami P, Zhang Z, et al. A novel method for quantifying the in-vivo mechanical effect of material injected into a myocardial infarction. Ann Thorac Surg. 2011; 92:935–41. [PubMed: 21871280]

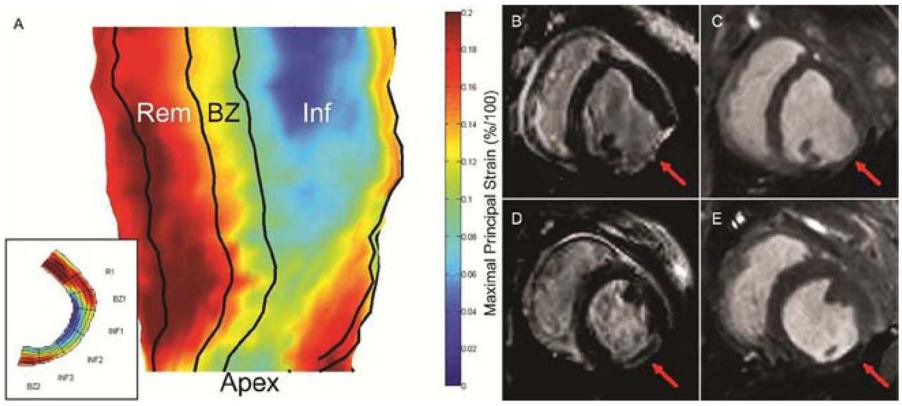

Figure 1.

(A) 3D radial strain map generated from manually segmented mid-myocardial contours. 2D short-axis strain maps (inset) are first generated for each myocardial slice from apex to base. Infarct, borderzone, and remote boundaries are then identified. Inf – Infarct region, BZ – Borderzone region, Rem – Remote region, Apex – LV apex. (B–E) Late gadolinium enhanced and cine images of 4wk untreated control (B & C) and 4wk Radiesse® treated (D & E) infarcts at end diastole. Red arrow denotes infarct area. Diffuse Radiesse® deposits are visible within the infarct scar as a black void.

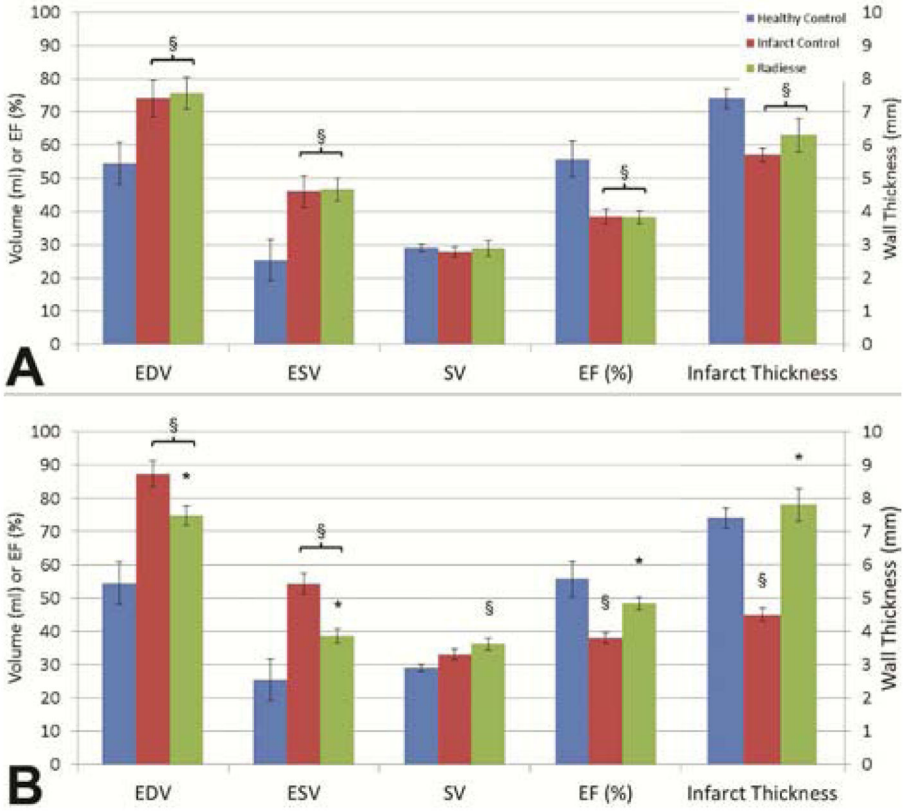

Figure 2.

Summary of LV global function indices (left axis) and *in vivo* posterolateral wall thickness (right axis) at both one (A) and four weeks (B) post-infarct in infarct control and Radiesse® treated groups compared to healthy control. § denotes $p<0.05$ vs healthy control, * denotes $p<0.05$ vs 4wk infarct control.

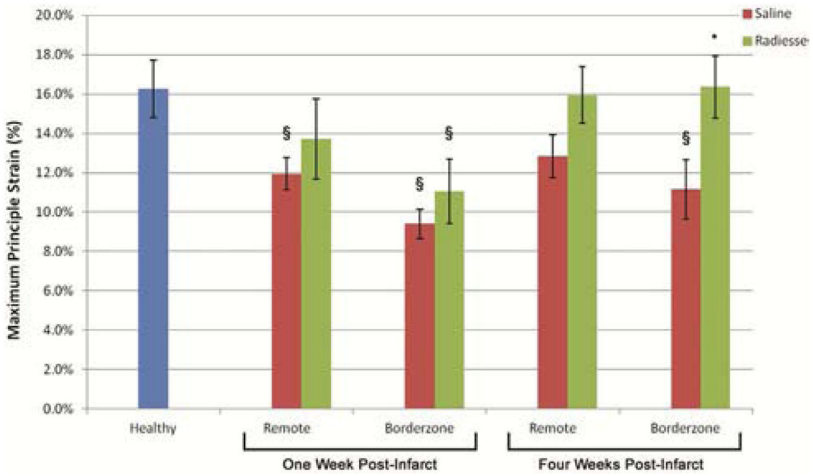

Figure 3.

Summary of regional radial strain (ε_{max}) at both one and four weeks post-infarct in infarct control and Radiesse® treated groups compared to healthy control. § denotes $p<0.05$ vs healthy control, * denotes $p<0.05$ vs 4wk infarct control borderzone myocardium.

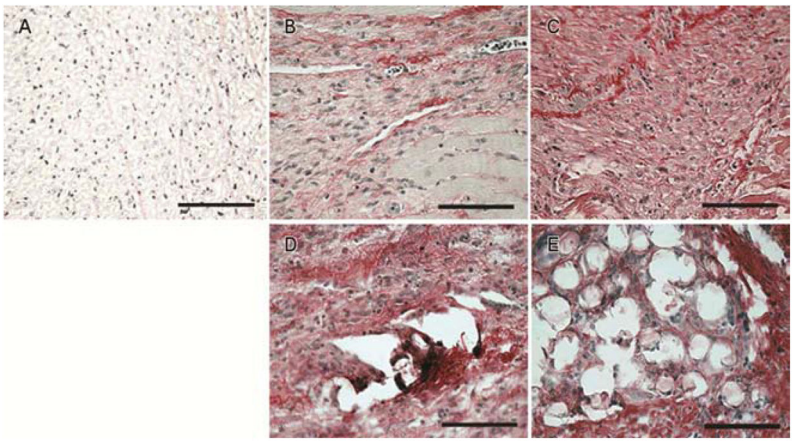

Figure 4.

PSR collagen staining of healthy (A), 1wk untreated (B), 4wks untreated (C), 1wk Radiesse® treated (D), and 4wks Radiesse® treated (E) infarcts. Dense collagen deposits and cellular infiltrates surrounded Radiesse® islands in treated infarcts. Collagen deposition was decreased and more homogenous in MI controls.